NIH Public Access
Author Manuscript
Biomaterials. Author manuscript; available in PMC 2010 October 1.

Published in final edited form as:
Biomaterials. 2009 October ; 30(30): 5910–5917. doi:10.1016/j.biomaterials.2009.06.034.

Scaffold-Free Vascular Tissue Engineering Using Bioprinting

Cyrille Norotte, Ph.D.[1], **Francoise Marga, Ph.D.**[1], **Laura Niklason, Ph.D.**[2], and **Gabor Forgacs, Ph.D.**[1,3,4,*]

[1]Department of Physics, University of Missouri, Columbia, MO 65211, USA

[2]Departments of Anesthesiology and Biomedical Engineering Yale University, New Haven, CT 06520 USA

[3]Department of Biology, University of Missouri, Columbia, MO 65211, USA

[4]Department of Biomedical Engineering, University of Missouri, Columbia, MO 65211, [1]USA

Abstract

Current limitations of exogenous scaffolds or extracellular matrix based materials have underlined the need for alternative tissue-engineering solutions. Scaffolds may elicit adverse host responses and interfere with direct cell-cell interaction, as well as assembly and alignment of cell-produced ECM. Thus, fabrication techniques for production of scaffold-free engineered tissue constructs have recently emerged. Here we report on a fully biological self-assembly approach, which we implement through a rapid prototyping bioprinting method for scaffold-free small diameter vascular reconstruction. Various vascular cell types, including smooth muscle cells and fibroblasts, were aggregated into discrete units, either multicellular spheroids or cylinders of controllable diameter (300 to 500 μm). These were printed layer-by-layer concomitantly with agarose rods, used here as a molding template. The post-printing fusion of the discrete units resulted in single- and double-layered small diameter vascular tubes (OD ranging from 0.9 to 2.5 mm). A unique aspect of the method is the ability to engineer vessels of distinct shapes and hierarchical trees that combine tubes of distinct diameters. The technique is quick and easily scalable.

1. Introduction

The general model of most tissue-engineering strategies rests on the use of exogenous biocompatible scaffolds in which cells can be seeded and matured *in vitro* or *in vivo*, to grow the tissue of interest. Scaffolds have been subject to prolific research and development over the last thirty years and, in general, offer the advantage of good biocompatibility, cell attachment and proliferation, while providing the biological, chemical, and mechanical clues to guide the eventual cell differentiation and assembly into a 3D tissue construct. Scaffold-based tissue engineering has led to significant results in the reconstruction of various tissues and organs and, in some cases, has been further translated to clinical practice [1-6].

Biomaterials-based solutions, though promising, still face general as well as specific challenges. Scaffold choice, immunogenicity, degradation rate, toxicity of degradation products, host inflammatory responses, fibrious tissue formation due to scaffold degradation, mechanical mismatch with the surrounding tissue are key issues, that may affect the long term

* Corresponding author: Tel.: +1 573 882 3036; fax: +1573 882 4195. *E-mail*: forgacsg@missouri.edu (G. Forgacs).

Publisher's Disclaimer: This is a PDF file of an unedited manuscript that has been accepted for publication. As a service to our customers we are providing this early version of the manuscript. The manuscript will undergo copyediting, typesetting, and review of the resulting proof before it is published in its final citable form. Please note that during the production process errors may be discovered which could affect the content, and all legal disclaimers that apply to the journal pertain.

NIH-PA Author Manuscript
NIH-PA Author Manuscript
NIH-PA Author Manuscript

NIH-PA Author Manuscript

NIH-PA Author Manuscript

NIH-PA Author Manuscript

behavior of the engineered tissue construct, and directly interfere with its primary biological function [7]. An example is myocardial tissue that presents high cell density necessary to assure synchronous beating through gap junctions that tightly interconnect neighboring cells. The use of scaffolds in cardiac tissue-engineering has been associated with reduced cell-to-cell connection, as well as incorrect deposition and alignment of extracellular matrix (ECM; i.e. collagen and elastin), affecting scaffold biodegradation and the force-generating ability of myocardial constructs [8,9]. ECM-related factors are particularly critical in vascular tissue engineering. Largely for this reason the promise of a scaffold-engineered small-diameter blood vessel substitute with mechanical strength comparable to native vessels for adult arterial revascularization, often described as the “holy grail” of tissue-engineering, remains unrealized. Besides the recurrent difficulty to produce elastic fibers *in vitro* [10], the use of scaffolds presents additional problems. The inherent weakness of the gels may hinder the final strength of the tissue-engineered vessel [11]. The presence of residual polymer fragments can disrupt the normal organization of the vascular wall [12,13] and even influence smooth muscle cell (SMC) phenotype [14]. Therefore it is not surprising that the first clinical applications of tissue-engineered vascular grafts have either targeted low-pressure applications [4] or relied on an entirely scaffold-free method termed sheet-based tissue-engineering [15-18] (currently under study also for myocardial reconstruction [19]).

A variety of techniques have been developed to engineer tissues without any scaffold, composed only of cells and the matrix they secrete. Such techniques are being applied even in areas where scaffolds have had early success such as the engineering of skin, bone or cartilage [20-22]. Despite these developments, scaffold-free tissue-engineering has yet to provide a reliable method to produce custom-shaped tissues in a reproducible, high throughput and easily scalable fashion while keeping precise control of pattern formation, particularly in case of multiple cell types.

To address some of the present challenges, we have recently introduced a rapid prototyping technology based on three-dimensional, automated, computer-aided deposition of “bioink particles” (multicellular spheroids) into a “biopaper” (biocompatible gel; e.g. collagen) by a bioprinter [23,24]. Three dimensional tissue structures such as myocardial patches were formed through the post-printing fusion of the bioink particles similar to self-assembly phenomena in early morphogenesis [25]. Delivery of bioink particles with this technology was rapid, accurate and assured maximal cell density, while showing minimal cell damage that is often associated with other solid freeform fabrication-based deposition methods [26-30] focused mostly on printing cells in combination with hydrogels. The success of the reported technology depended strongly on the collagen biopaper [23,31]. Collagen gelation time was critical for the smooth deposition of the multicellular spheroids. Collagen concentration had to be finely tuned to assure the fusion of the spheroids during the postprinting phase [31]. Layer-by-layer construction lacked precision beyond a few layers due to progressive distortion of the construct, caused by the uneven gelation of successive collagen sheets [23]. Biopaper removal after postprinting fusion was technically challenging. As some of the supporting collagen was incorporated within the construct during the fusion of the spheroids, this method was indeed not entirely scaffold free.

In the present study, we describe and employ a fully biological scaffold-free tissue engineering technology and apply it to fabricate small-diameter multi-layered tubular vascular grafts that are readily perfusable for further maturation. We show that the approach circumvents a number of shortcomings associated with scaffolds and achieves the goal of being rapid, reproducible, and easily scalable by means of rapid prototyping.

NIH-PA Author Manuscript
NIH-PA Author Manuscript
NIH-PA Author Manuscript

2. Materials and Methods

2.1. Cell Culture

Chinese Hamster Ovary (CHO) cells transfected with N-cadherin were grown in Dulbecco's Modified Eagle Medium (DMEM; Invitrogen, Carlsbad, CA) supplemented with 10% Fetal Bovine Serum (FBS; Atlanta Biologicals, Lawrenceville, GA), antibiotics (100U/mL penicillin streptomycin and 25 μg/mL gentamicin) and 400 μg/ml geneticin. Besides gentamicin (American Pharmaceutical Partners, IL) all antibiotics were purchased from Invitrogen. Human umbilical vein smooth muscle cells (HUVSMCs) and Human skin fibroblasts (HSFs) were purchased from the American Type Culture Collection (CRL-2481 and CRL-2522 respectively; ATCC, Manassas, VA). HUVSMCs were grown in DMEM with Ham's F12 (Invitrogen) in ratio 3:1, 10% FBS, antibiotics (100U/mL penicillin-streptomycin and 25 ug/mL gentamicin), 20 μg/mL Endothelial Cell Growth Supplement (ECGS; Upstate, Lake Placid, NY), Sodium Pyruvate (NaPy; Invitrogen) 0.1M. Human skin fibroblasts (HSFs) were grown in DMEM with Ham's F12 in ratio 3:1, 20% FBS, antibiotics (100U/mL penicillin/streptomycin and 25 μg/mL gentamicin), glutamine 2mM, NaPy 0.1M. Freshly isolated porcine aortic smooth muscle cells (PASMCs) were grown in low glucose DMEM with 10% FBS (Hyclone Laboratories, UT), 10% porcine serum (Invitrogen), L-ascorbic acid, copper sulfate, HEPES, L-proline, L-alanine, L-glycine, and Penicillin G (all aforementioned supplements were purchased from Sigma, St. Louis, MO). All cell lines were cultured on 0.5% gelatin (porcine skin gelatin; Sigma) coated dishes (Techno Plastic Products, St. Louis, MO) and were maintained at 37°C in a humidified atmosphere containing 5% CO_2.

2.2. Preparation of multicellular spheroids and cylinders and agarose rods

Cell cultures were washed twice with phosphate buffered saline solution (PBS, Invitrogen) and treated for 10 min with 0.1% Trypsin (Invitrogen) and centrifuged at 1,500 RPM for 5 min. Cells were resuspended in 4 ml of cell-type specific medium and incubated in 10-ml tissue culture flasks (Bellco Glass, Vineland, XNJ) at 37°C with 5% CO_2 on gyratory shaker (New Brunswick Scientific, Edison, NJ) for one hour, for adhesion recovery and centrifuged at 3,500 RPM. The resulting pellets were transferred into capillary micropipettes of 300 μm (Sutter Instrument, CA) or 500 μm (Drummond Scientific Company, Broomall, PA) diameters and incubated at 37°C with 5% CO_2 for 15 min. For spherical bioink, extruded cylinders were cut into equal fragments that were let to round up overnight on a gyratory shaker. Depending on the diameter of the micropipettes, this procedure provided regular spheroids of defined size and cell number (Fig. 1). For cylindrical bioink, cylinders were mechanically extruded into specifically prepared non-adhesive Teflon or agarose molds using the bioprinter (Fig. 2A,B). After overnight maturation in the mold, cellular cylinders were cohesive enough to be deposited.

To prepare agarose rods, liquid agarose (temperature > 40^0C) was loaded into micropipettes (300 or 500 μm ID). Loaded micropipettes were immersed into cold PBS (4^0C). As agarose did not adhere to the micropipette, upon gelation, continuous rods could easily be extruded by the bioprinter using another printing head (Fig. 5C; cf. with Fig. 2A).

2.3. Imaging and visualization

The morphology of multicellular spheroids was analyzed by FESEM (Field Emission Scanning Electron Microscopy). Spheroids were fixed in 4% paraformaldehyde (Electron Microscopy Sciences, Hatfield, PA) in phosphate-buffered saline (PBS) for 90 min, on a low speed shaker. Subsequently, samples were rinsed 3 times for 10 min in PBS. Dehydration was performed by an increasing concentration series of ethanol as follows: 10%, 25%, 50%, 75%, 95%, for 30 min each and finally in 100% ethanol overnight. After critical point drying (in Tousumis Samdri-PVT-3B; Tousimis, Rockville, MD), aggregates were spread on carbon adhesive tabs

NIH-PA Author Manuscript

NIH-PA Author Manuscript

NIH-PA Author Manuscript

mounted on stub and sputter coated with platinum to a nominal thickness of 2 nm. Aggregate surface was examined using a Hitachi S4700 cold-cathode field-emission scanning electron microscope at an accelerating voltage of 5 kV.

To visualize the fusion of multicellular spheroids, cells were stained with green or red membrane-intercalating dyes (SP-DilC18 and SP-DiOC18; Molecular Probes, Eugene, OR) according to the protocol supplied by the manufacturer. Cells were replated after labeling to recover from the staining procedure and then used to make multicellular spheroids of different fluorescent colors. Fusion patterns were monitored using a fluorescence stereomicroscope (Leica, Bannockburn, IL).

2.4. Immunohistochemistry

Tissues were fixed overnight in 4% paraformaldehyde. After dehydration, tissues were processed for paraffin infiltration and embedding. 5 For global aspect μm sections were stained with hematoxylin-eosin. For immunohistochemistry sections were incubated with the following antibodies: anti-cleaved caspase-3 (1:50 dilution of a rabbit anti-cleaved caspase-3 polyclonal antibody that reacts with mouse and human cleaved caspase-3, Trevigen, MD); anti-smooth muscle actin (1:400 dilution of a mouse anti-human smooth muscle actin (1A4; Dako, Carpinteria, CA). Secondary antibodies (EnVision+, a horseradish peroxidase–labeled polymer conjugated with either anti-mouse or anti-rabbit antibodies; Dako) were visualized using DAB (3’-diaminobenzidine tetrahydrochloride). Sections were counterstained with Mayer's hematoxylin, and coverslipped for microscopic examination (IX70; Olympus, Center Valley, PA).

3. Results

3.1. Scaffold-free, macrovascular tubular structures built of multicellular spheroids

To assemble tissue spheroids into customized tubular structures of defined topology, we designed a scaffold-free approach based on the use of agarose rods as building blocks of a molding template (Fig. 3). When agarose rods and uniform multicellular spheroids were deposited layer-by layer, this template allowed for the accurate control of tube diameter, wall thickness and branching pattern (Fig. 3).

Using this approach, straight tubes were initially built manually, according to patterns in Fig. 3A-H. The smallest tube was assembled according to the simplest pattern (Fig. 3A-E) and was 900 μm in diameter with a wall thickness of 300 μm (Fig. 4A). Once assembled, multicellular spheroids fused within 5 to 7 days to result in the final tubular construct. To study the fusion process in more detail, spheroids, with their composing cells stained with either green or red membrane dyes, were assembled according to the scheme shown in Fig 3E. Fusion of alternate sequences of green and red spheroids is shown in Fig. 4B and reveals a sharp fusion boundary with little intermingling, confirming earlier findings [32].

In addition to flexibility in tube diameter and wall thickness, the presented method, as its unique feature, provides a way to construct branched macrovascular structures. For this purpose, to ensure correct luminal connection, the different branches of the vascular tree were assembled simultaneously. Branched tubular structures of distinct diameters (Fig. 4C) were built according to the pattern in Fig. 3I. Spheroids fused in 5 to 7 days (Fig. 4D).

Despite the relative simplicity of this scaffold-free approach, we noticed several deficiencies, most of them associated with the use of spheroids as building blocks. Preparation of large quantities of spheroids (> 1000) necessary to build larger and longer tubes is time-consuming. Fusion of the spheroids may take as long as a week and lead to non-uniform tubular surfaces

NIH-PA Author Manuscript

NIH-PA Author Manuscript

NIH-PA Author Manuscript

(Fig. 4D). Finally, assembling tubular constructs manually in a sterile fashion, albeit possible, is challenging.

3.2. Using multicellular cylinders as building-blocks for vascular tissue-engineering

Preparation of tubular constructs by the above approach served as proof of principle. Next we sought to adapt the method to potential clinical applications, and thus also to rapid prototyping to gain in speed, precision and reproducibility. For this, we adapted the specifically built three-dimensional delivery device in Fig. 1 for the deposition of agarose rods and multicellular cylinders, keeping the same conceptual approach described above (Fig. 5).

3.3. Printing single and double-layered vascular tubes

One of the advantages of using cylindrical units is that with these bioink particles the scheme shown in Fig. 3 can be automated. Indeed, the computer-aided rapid prototyping bioprinting technology, illustrated in Fig. 5 allowed for the controlled, simultaneous deposition of the agarose rods and multicellular cylinders according to the same templates as before (cf. Fig. 3E and 5A,B). (Printing spherical bioink particles albeit possible [23], is considerably more cumbersome.) Deposition was carried out by the same bioprinter used for the preparation of the cylindrical bionk, now equipped with two print heads, one for the preparation and extrusion of agarose rods, the other for the deposition of multicellular cylinder (Fig. 5C). Loading, gelation and extrusion of agarose rods took place in a fully automated cycle. The micropipette-cartridge attached to the print head was first moved to a warm liquid agarose vial for loading. Next, to allow for the rapid gelation of agarose, the loaded cartridge was immersed in a cold PBS vial. Finally, the resulting agarose rod was extruded into a Petri Dish (see Supplementary Video1). When the deposition scheme called for the delivery of a multicellular cylinder, one such cylinder was drawn from the agarose mold (Fig. 1B) into a micropipette. The micropipette was then loaded into the second print head and the cellular cylinder extruded similarly to an agarose rod. Simple straight tubes of HUSMCs were printed according to the design shown in Fig. 5A (cf. with Fig. 3A-E and see Supplementary Video 2). The computer-aided motion and coordination of the two print heads assured the reproducibility of the pre-programmed pattern. After assembly (Fig. 5B,D), the multicellular cylinders fused within two to four days into the final tubular structure, and the supporting agarose rods were removed (Fig. 5F).

Next we constructed double-layered vascular tubes similar to vessels in the macrovasculature with a media and adventitia. For this we used both HUSMC and HSF cylinders as building blocks according to the pattern shown in Fig. 6A. To show the versatility of the method, we also engineered tubes by alternatively depositing multicellular cylinders composed of HUSMCs and HSF (Fig. B), a pattern that has no in vivo equivalent. Hematoxilin-eosin (H&E) (Fig. 6F,F) and smooth muscle actin staining of HUSMCs (Fig. 6D,G) indicated a sharp boundary between the SMC and fibroblast layers or regions in the engineered constructs after 3 days of fusion. Caspase 3 staining revealed a few apoptotic cells in the wall (Fig. 6E,H).

4. Discussion

This study describes an approach to build scaffold-free vascular constructs of defined cellular composition and geometry. Linear and branched tubular structures were engineered using various cell types. Parameters such as size, wall thickness or cell patterning were adjusted to arrive at single- or double-layered tubes ranging from 0.9 to 2.5 mm in outer diameter. The method avoids a number of the general shortcomings associated with exogenous materials and offers specific advantages. As engineered constructs are built from cells only, the highest possible cell density is achieved, a challenge when scaffolds are employed [33]. This is important as native vessels present a relatively cell-dense media layer with overlapping adjacent SMCs [34]. The presented technology uses multicellular three-dimensional spheroids

NIH-PA Author Manuscript

NIH-PA Author Manuscript

NIH-PA Author Manuscript

or cylinders as building blocks and thus relies on self-adhering cell types. We have previously quantified tissue cohesion through cell-cell interaction by analogy with liquid systems, and reported that SMCs represent one of the most self-cohesive cell type ever observed [35]. The analogy between multicellular assemblies and liquids [36] provided a better understanding of some of the developmental morphogenetic processes employed here. Rounding or fusion of multicellular spheroids and cylinders described in this study (Figs. 2,4-6) are consistent with the physical understanding that, on a time scale of hours, tissues composed of motile and adhesive cells mimic highly viscous, incompressible liquids, a concept previously exploited for tissue-engineering [23,25].

We first tested the new method with multicellular spheroids of distinct size (300 μm or 500 μm), which (compared to approaches for scaffold-free aggregation of cells into spheroids [20,25,37]), we are able to fabricate reliably and reproducibly. However the use of tissue spheroids as building blocks still had limitations. The fusion process was long and led to a somewhat inhomogeneous construct (Fig. 4D). Building long vascular tubes was labor- and spheroid-intensive: about 4,000 spheroids of 300 μm were needed to fabricate a 10 cm long, 1.5 mm OD tube by the scheme in Fig. 3H. Therefore we sought to develop a more rapid, high throughput method for engineering vascular tubes, while keeping the same scaffold-free design concept. Instead of spheroids we used multicellular cylinders as bioink (up to 7cm in length), and bioprinting as a rapid prototyping technology. A three-dimensional computer-controlled delivery device (i.e. bioprinter) was employed in the different phases of the tube-fabrication process. When the bioprinter was equipped with a microcapillary attachment module it facilitated the automated, speedy, accurate and simultaneous deposition of freshly prepared (and thus weak) multicellular cylinders into the maturation agarose mold (Fig. 2). Overnight maturation of the cylinders allowed to recover tissue cohesion and prevented distortion of the cylinders, before their actual layer-by-layer deposition. The same printer, with a different module was used for the actual building of various tubular structures. Post-printing fusion of the cellular cylinders was significantly more rapid (2 to 4 days), than of spheroids, and led to the formation of uniform tubes without any visible macroscopic defaults (Fig. 5E). The fused products were sufficiently sturdy to be handled and transferred into specifically designed bioreactors for further maturation (presently under way) to acquire the necessary mechanical properties for implantation (Fig. 7). Compared to tissue spheroids, the use of multicellular cylinders represents considerable progress in terms of time and precision of the final structure.

In the classic approach, the final geometry of the engineered tissue or organ are controlled by scaffolds of predetermined size and shape [38]. Here we demonstrated that customized scaffold-free vascular tubes can be engineered according to simple design templates (Fig. 3).

A current limitation of the presented method is the spatial resolution of the final construct, here the thickness of the vascular wall. In this study we used micropipettes of relatively large diameter (300 or 500 μm) for the preparations and deposition of agarose and cellular cylinders. As a consequence, we observed sparsely distributed apoptotic cells throughout the vascular wall (Fig. 6E, H) after 3 days of fusion. Although the apoptotic pattern does not seem to be depth-dependent, it is known that diffusion of nutrients and oxygen is limited to a few hundred microns in in vitro engineered tissues [39]. To survive, most tissues need to be vascularized. Creating a vascular supply system in thick tissue-engineered constructs remains a major challenge [40]. Recent studies have shown the ability to fabricate microvascular networks in vitro, leading to the production of various prevascularized bioengineered tissues [41-44]. Despite these advances, viability upon implantation remains problematic as infiltration of surrounding vessels or connection of microvascularized constructs with the host vasculature takes days to weeks, predisposing the tissue to ischemia [45]. The ability to create constructs containing a complex hierarchical macro- to micro-vascular tree in vitro will be a significant

NIH-PA Author Manuscript

NIH-PA Author Manuscript

NIH-PA Author Manuscript

step towards the engineering of complex tissues. The method presented here is an attempt in this direction (Fig. 4D).

Due to resolution limitations, the smallest tube diameter we can currently build has 900 μm OD. Using smaller micropipettes and their combinations for the preparation of multicellular cylinders should make it possible to narrow the tube diameter and wall thickness (e.g. using 100 μm micropipettes would lead to 300 μm tubes with 100 μm wall thickness). Thinner vascular wall would lead to better cell viability.

Another issue relates to the removal of the agarose rods that occupy the lumen of the branched tubes when the geometry becomes more complex. This is currently achieved by manually pulling the agarose rods out of the tube, a procedure that limits the geometry of the final vascular tree: its branches have to be open-ended (Fig. 4D). Use of other (e.g. thermoreversible, photosensitive) molding gels would eliminate this limitation.

Vascular patterning remains a major challenge for small-diameter blood vessel tissue-engineering, mainly due to the number and precise position of the vascular cell types within the vessel wall. Small-caliber blood vessels are typically composed of three layers: an inner intima, a thick, dense media, and an outer adventitia, respectively populated by endothelial cells (EC), SMCs, and fibroblasts. While the inner endothelial monolayer can be quickly constructed by EC seeding prior to implantation [46], seeding different cell types at precise locations within a single scaffold remains a challenge [13]. Initial positioning of the various cell types is straightforward in the presented method, as demonstrated by the double-layered tube with its inner and outer layer composed respectively of SMCs and fibroblasts (Fig. 6).

5. Conclusions

We built fully biological vascular tubular grafts by employing a rapid prototyping method. As the approach allows for easy patterning of distinct cell types we were able to construct structures that are both compositionally and architecturally intricate. In particular we engineered tubes of multiple layers and complex branching geometry. The method represents a scaffold-free tissue fabrication technology that is accurate, reliable and scalable. It is not restricted to tubular biological structures.

Supplementary Material

Refer to Web version on PubMed Central for supplementary material.

Acknowledgement

Authors wish to thank Mr. Liping Zhao for technical assistance on porcine smooth muscle cell culture. Support for this research was provided by the National Institutes of Health (R01 HL-083895 to L. N.) and the National Science Foundation FIBR program (EF-0526854 to GF).

REFERENCES

1. Atala A, Bauer SB, Soker S, Yoo JJ, Retik AB. Tissue-engineered autologous bladders for patients needing cystoplasty. Lancet 2006;367:1241–1246. [PubMed: 16631879]
2. Kerker JT, Leo AJ, Sgaglione NA. Cartilage repair: synthetics and scaffolds: basic science, surgical techniques, and clinical outcomes. Sports Med Arthrosc 2008;16:208–216. [PubMed: 19011552]
3. Priya SG, Jungvid H, Kumar A. Skin tissue engineering for tissue repair and regeneration. Tissue Eng Part B Rev 2008;14:105–218. [PubMed: 18454637]
4. Shin'oka T, Imai Y, Ikada Y. Transplantation of a tissue-engineered pulmonary artery. N Engl J Med 2001;344:532–533. [PubMed: 11221621]

NIH-PA Author Manuscript

NIH-PA Author Manuscript

NIH-PA Author Manuscript

5. van Tienen TG, Hannink G, Buma P. Meniscus replacement using synthetic materials. Clin Sports Med 2009;28:143–156. [PubMed: 19064171]
6. Lee K, Chan CK, Patil N, Goodman SB. Cell therapy for bone regeneration-Bench to bedside. J Biomed Mater Res B Appl Biomater 2008;89:252–263. [PubMed: 18777578]
7. Williams DF. On the mechanisms of biocompatibility. Biomaterials 2008;29:2941–2953. [PubMed: 18440630]
8. Shimizu T, Yamato M, Kikuchi A, Okano T. Cell sheet engineering for myocardial tissue reconstruction. Biomaterials 2003;24:2309–2316. [PubMed: 12699668]
9. Zimmermann WH, Didie M, Doker S, Melnychenko I, Naito H, Rogge C, et al. Heart muscle engineering: an update on cardiac muscle replacement therapy. Cardiovasc Res 2006;71:419–429. [PubMed: 16697358]
10. Patel A, Fine B, Sandig M, Mequanint K. Elastin biosynthesis: The missing link in tissue-engineered blood vessels. Cardiovasc Res 2006;71:40–49. [PubMed: 16566911]
11. Weinberg CB, Bell E. A blood vessel model constructed from collagen and cultured vascular cells. Science 1986;231:397–400. [PubMed: 2934816]
12. Dahl SL, Rhim C, Song YC, Niklason LE. Mechanical properties and compositions of tissue engineered and native arteries. Ann Biomed Eng 2007;35:348–355. [PubMed: 17206488]
13. Iwasaki K, Kojima K, Kodama S, Paz AC, Chambers M, Umezu M, et al. Bioengineered three-layered robust and elastic artery using hemodynamically-equivalent pulsatile bioreactor. Circulation 2008;118:S52–S57. [PubMed: 18824769]
14. Higgins SP, Solan AK, Niklason LE. Effects of polyglycolic acid on porcine smooth muscle cell growth and differentiation. J Biomed Mater Res A 2003;67:295–302. [PubMed: 14517889]
15. L'Heureux N, Paquet S, Labbe R, Germain L, Auger FA. A completely biological tissue-engineered human blood vessel. Faseb J 1998;12:47–56. [PubMed: 9438410]
16. L'Heureux N, McAllister TN, de la Fuente LM. Tissue-engineered blood vessel for adult arterial revascularization. N Engl J Med 2007;357:1451–1453. [PubMed: 17914054]
17. Konig G, McAllister TN, Dusserre N, Garrido SA, Iyican C, Marini A, et al. Mechanical properties of completely autologous human tissue engineered blood vessels compared to human saphenous vein and mammary artery. Biomaterials 2009;30:1542–1550. [PubMed: 19111338]
18. McAllister TN, Maruszewski M, Garrido SA, Wystrychowski W, Dusserre N, Marini A, et al. Effectiveness of haemodialysis access with an autologous tissue-engineered vascular graft: a multicentre cohort study. Lancet 2009;373:1440–1446. [PubMed: 19394535]
19. Masuda S, Shimizu T, Yamato M, Okano T. Cell sheet engineering for heart tissue repair. Adv Drug Deliv Rev 2008;60:277–285. [PubMed: 18006178]
20. Kelm JM, Fussenegger M. Microscale tissue engineering using gravity-enforced cell assembly. Trends Biotechnol 2004;22:195–202. [PubMed: 15038925]
21. Auxenfans C, Fradette J, Lequeux C, Germain L, Kinikoglu B, Bechetoille N, et al. Evolution of three dimensional skin equivalent models reconstructed in vitro by tissue engineering. Eur J Dermatol 2008;19:107–113. [PubMed: 19106039]
22. Matsusaki M, Kadowaki K, Tateishi K, Higuchi C, Ando W, Hart DA, et al. Scaffold-Free Tissue-Engineered Construct-Hydroxyapatite Composites Generated by an Alternate Soaking Process: Potential for Repair of Bone Defects. Tissue Eng Part A 2009;15:55–63. [PubMed: 18673091]
23. Jakab K, Norotte C, Damon B, Marga F, Neagu A, Besch-Williford CL, et al. Tissue engineering by self-assembly of cells printed into topologically defined structures. Tissue Eng Part A 2008;14:413–421. [PubMed: 18333793]
24. Neagu A, Jakab K, Jamison R, Forgacs G. Role of physical mechanisms in biological self-organization. Phys Rev Lett 2005;95:178104. [PubMed: 16383876]
25. Marga F, Neagu A, Kosztin I, Forgacs G. Developmental biology and tissue engineering. Birth Defects Res C Embryo Today 2007;81:320–328. [PubMed: 18228266]
26. Chang R, Nam J, Sun W. Effects of dispensing pressure and nozzle diameter on cell survival from solid freeform fabrication-based direct cell writing. Tissue Eng Part A 2008:1441–48.
27. Boland T, Xu T, Damon B, Cui X. Application of inkjet printing to tissue engineering. Biotechnol J 2006;1:910–917. [PubMed: 16941443]

NIH-PA Author Manuscript

NIH-PA Author Manuscript

NIH-PA Author Manuscript

28. Xu T, Jin J, Gregory C, Hickman JJ, Boland T. Inkjet printing of viable mammalian cells. Biomaterials 2005;26:93–99. [PubMed: 15193884]
29. Saunders RE, Gough JE, Derby B. Delivery of human fibroblast cells by piezoelectric drop-on-demand inkjet printing. Biomaterials 2008;29:193–203. [PubMed: 17936351]
30. Nahmias Y, Odde DJ. Micropatterning of living cells by laser-guided direct writing: application to fabrication of hepatic-endothelial sinusoid-like structures. Nat Protoc 2006;1:2288–2296. [PubMed: 17406470]
31. Jakab K, Neagu A, Mironov V, Markwald RR, Forgacs G. Engineering biological structures of prescribed shape using self-assembling multicellular systems. Proc Natl Acad Sci U S A 2004;101:2864–2869. [PubMed: 14981244]
32. Jakab K, Damon B, Marga F, Doaga O, Mironov V, Kosztin I, et al. Relating cell and tissue mechanics: implications and applications. Dev Dyn 2008;237:2438–2449. [PubMed: 18729216]
33. Martin I, Wendt D, Heberer M. The role of bioreactors in tissue engineering. Trends Biotechnol 2004;22:80–86. [PubMed: 14757042]
34. O'Connell MK, Murthy S, Phan S, Xu C, Buchanan J, Spilker R, et al. The three-dimensional micro- and nanostructure of the aortic medial lamellar unit measured using 3D confocal and electron microscopy imaging. Matrix Biol 2008;27:171–181. [PubMed: 18248974]
35. Norotte C, Marga F, Neagu A, Kosztin I, Forgacs G. Experimental evaluation of apparent tissue surface tension based on the exact solution of the Laplace equation. EPL (Europhysics Letters) 2008;81:46003.
36. Steinberg, MS.; Poole, T. Liquid behavior of embryonic tissues.. In: Bellair, R.; Curtis, ASG., editors. Cell Behavior. Liquid behavior of embryonic tissues. Cambridge University Press; Cambridge: 1982. p. 583-607.
37. Lin RZ, Chang HY. Recent advances in three-dimensional multicellular spheroid culture for biomedical research. Biotechnol J 2008;9−10:1172–1184.
38. Cao Y, Vacanti JP, Paige KT, Upton J, Vacanti CA. Transplantation of chondrocytes utilizing a polymer-cell construct to produce tissue-engineered cartilage in the shape of a human ear. Plast Reconstr Surg 1997;100:297–302. [PubMed: 9252594]
39. Muschler GF, Nakamoto C, Griffith LG. Engineering principles of clinical cell-based tissue engineering. J Bone Joint Surg Am 2004;86-A:1541–1558. [PubMed: 15252108]
40. Ko HC, Milthorpe BK, McFarland CD. Engineering thick tissues--the vascularisation problem. Eur Cell Mater 2007;14:1–18. [PubMed: 17654452]
41. Black AF, Berthod F, L'Heureux N, Germain L, Auger FA. In vitro reconstruction of a human capillary-like network in a tissue-engineered skin equivalent. Faseb J 1998;12:1331–1340. [PubMed: 9761776]
42. Unger RE, Sartoris A, Peters K, Motta A, Migliaresi C, Kunkel M, et al. Tissue-like self-assembly in cocultures of endothelial cells and osteoblasts and the formation of microcapillary-like structures on three-dimensional porous biomaterials. Biomaterials 2007;28:3965–3976. [PubMed: 17582491]
43. Levenberg S, Rouwkema J, Macdonald M, Garfein ES, Kohane DS, Darland DC, et al. Engineering vascularized skeletal muscle tissue. Nat Biotechnol 2005;23:8798–84.
44. Caspi O, Lesman A, Basevitch Y, Gepstein A, Arbel G, Habib IH, et al. Tissue engineering of vascularized cardiac muscle from human embryonic stem cells. Circ Res 2007;100:263–272. [PubMed: 17218605]
45. Rouwkema J, Rivron NC, van Blitterswijk CA. Vascularization in tissue engineering. Trends Biotechnol 2008;26:434–441. [PubMed: 18585808]
46. Alobaid N, Salacinski HJ, Sales KM, Hamilton G, Seifalian AM. Single stage cell seeding of small diameter prosthetic cardiovascular grafts. Clin Hemorheol Microcirc 2005;33:209–226. [PubMed: 16215287]

NIH-PA Author Manuscript
NIH-PA Author Manuscript
NIH-PA Author Manuscript

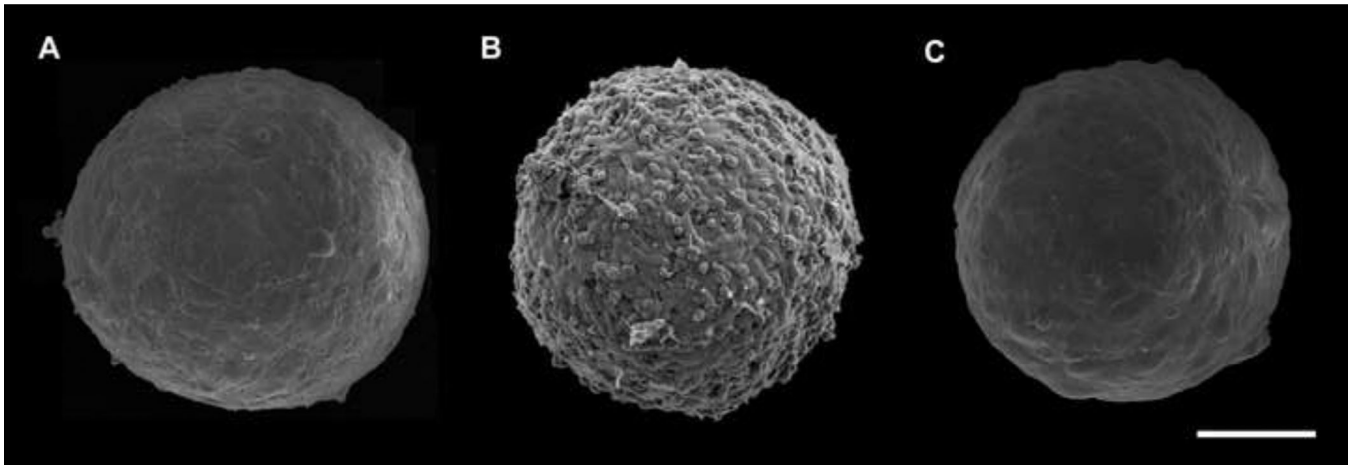

Fig. 1.

Scanning electron micrographs of 300 μm diameter multicellular spheroids of HUSMCs (A), CHO cells (B) and HFBs (C) employed in the present study. HUSMC and HSF spheroids display similar morphology with smooth and uniform surface and contain respectively about 8,000 and 15,000 cells. In contrast, CHO spheroids assume a berry-like shape suggesting that surface cells adhere more weakly to inner cell layers. Scale bar: 100 μm.

NIH-PA Author Manuscript
NIH-PA Author Manuscript
NIH-PA Author Manuscript

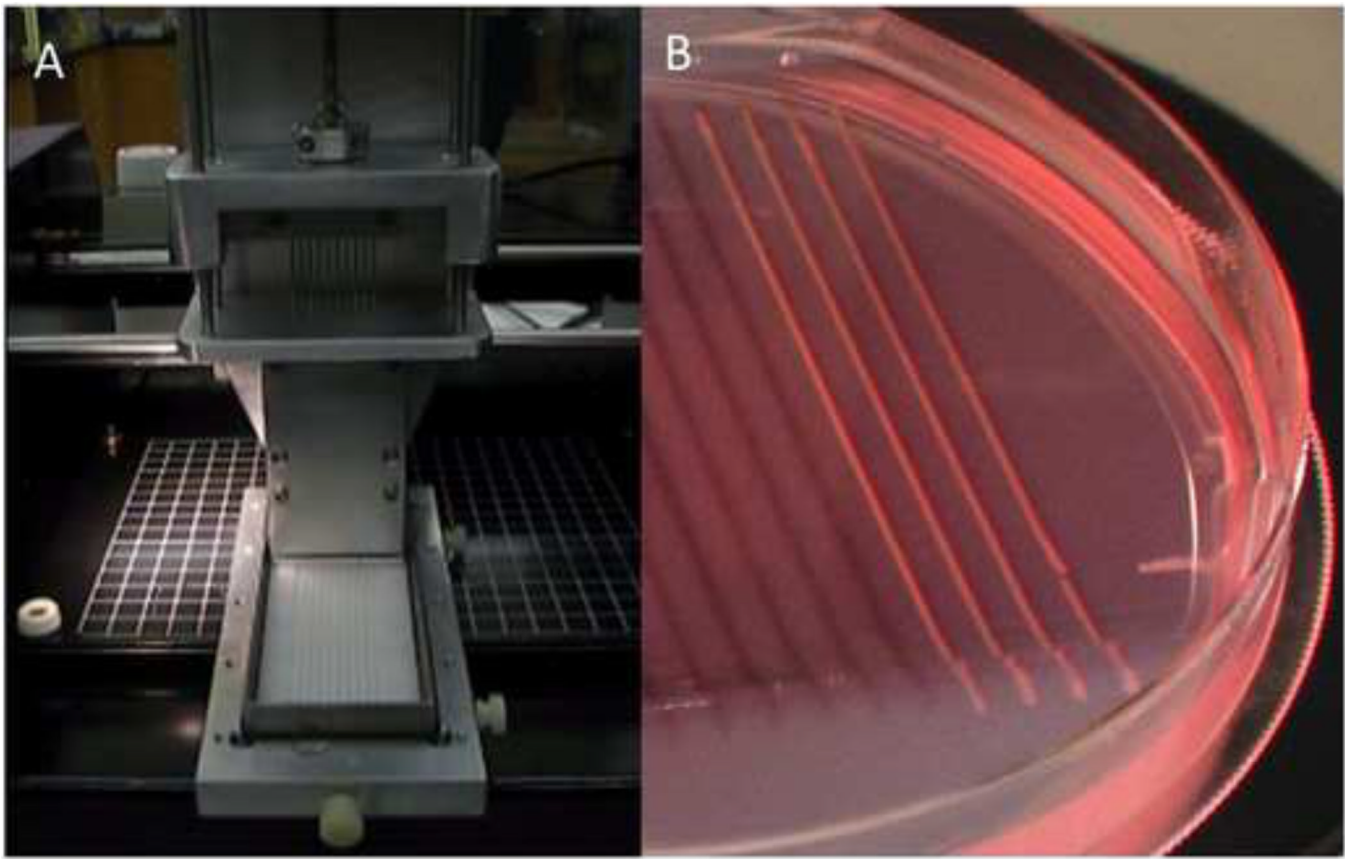

Fig. 2.
Preparation of cylindrical bioink. A. Upon cell aggregation in micropipettes, ten multicellular cylinders were simultaneously extruded using a special-purpose attachment to a specifically designed bioprinter. B. Non-adhesive agarose mold in which extruded cylinders were matured prior to be used as bioink.

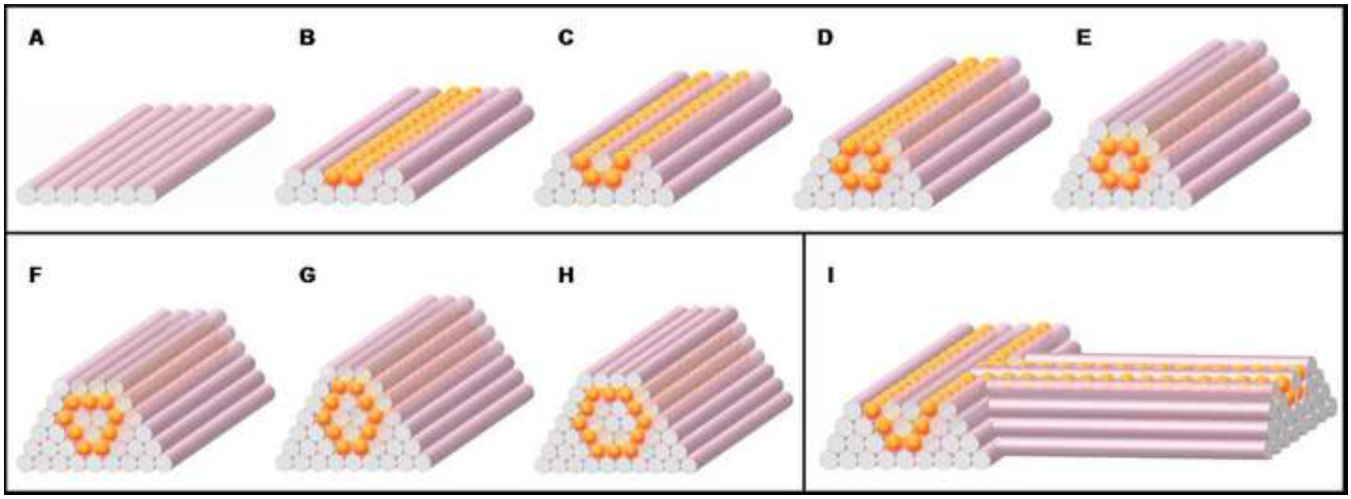

Fig. 3.
Design template for tubular structures. (A-E) Deposition scheme for the smallest diameter tube that can be built of agarose rods (pink) and multicellular spheroids (orange) of the same diameter. (F-H) More complex tubular structures. (I) Scheme for a branching structure.

NIH-PA Author Manuscript
NIH-PA Author Manuscript
NIH-PA Author Manuscript

NIH-PA Author Manuscript
NIH-PA Author Manuscript
NIH-PA Author Manuscript

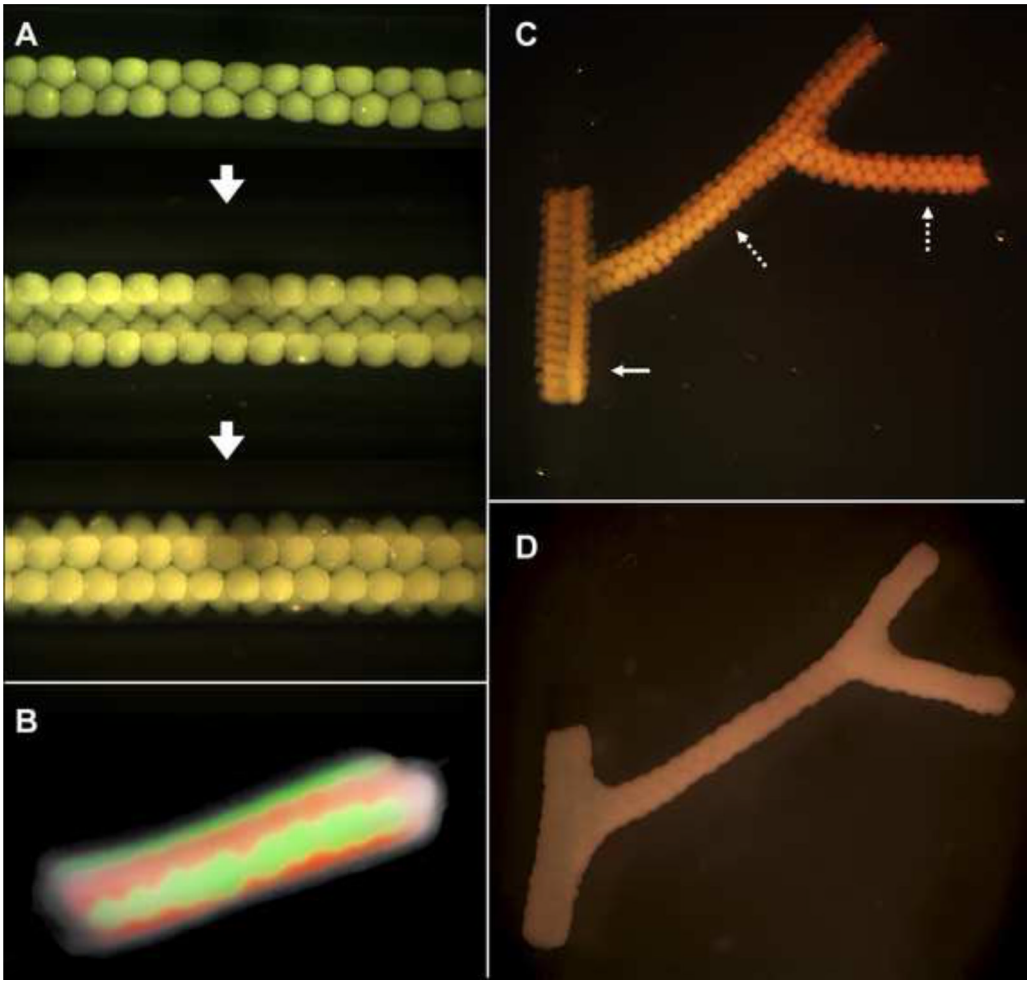

Fig. 4.

Fusion patterns of multicellular spheroids assembled into tubular structures. A. HSF spheroids assembled according to template in Fig. 3A-E. B. Fusion pattern after 7 days of a tube assembled from fluorescently labeled red and green sequences of CHO spheroids. C. Branched structure built of 300 μm HSF spheroids with branches of 1.2 mm (solid arrow) and 0.9 mm (broken arrows). D. The fused branched construct after 6 days of deposition.

NIH-PA Author Manuscript
NIH-PA Author Manuscript
NIH-PA Author Manuscript

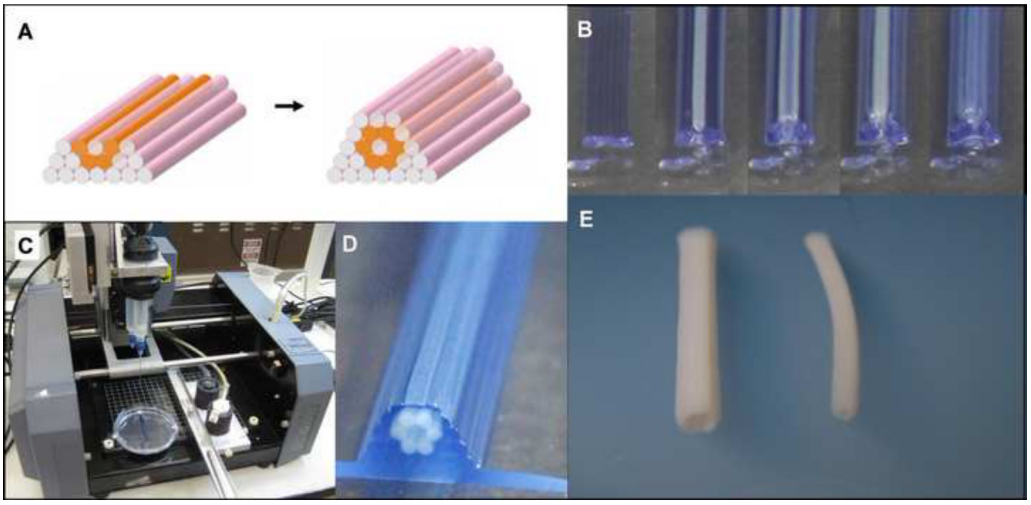

Fig. 5.

Bioprinting tubular structures with cellular cylinders. A. Design template analogous to the one in Fig. 3. B. Layer-by-layer deposition of agarose cylinders (stained here in blue for better visualization) and multicellular pig SMC cylinders. C. The bioprinter (see Materials and Methods) outfitted with two vertically moving print heads. D. The printed construct. E. Engineered pig SMC tubes of distinct diameters resulted after 3 days of post-printed fusion (left: 2.5 mm OD; right: 1.5 mm OD).

NIH-PA Author Manuscript

NIH-PA Author Manuscript

NIH-PA Author Manuscript

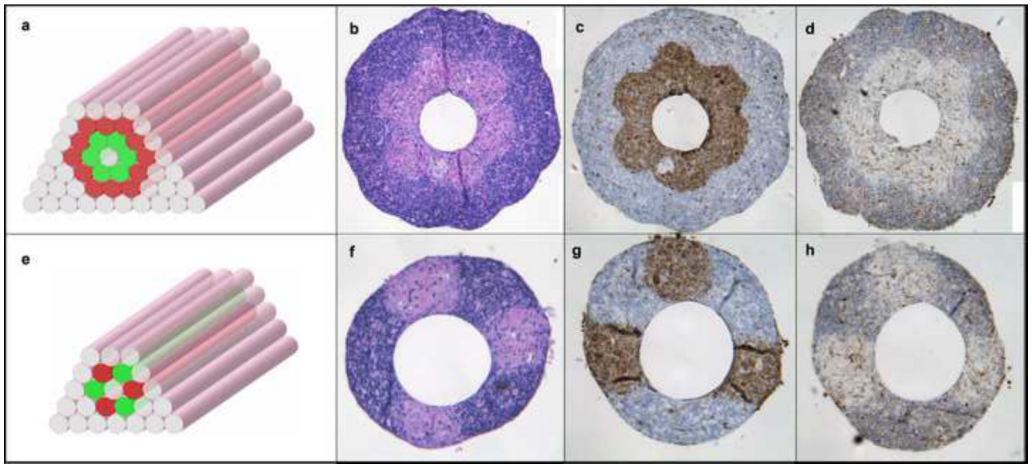

Fig. 6.

Building a double-layered vascular wall. A, B. HUVSMC and HSF multicellular cylinders were assembled according to specific patterns (HUVSMC: green; HSF: red) C-H. Histological examination of the structures after 3 days of fusion: H&E (C, F), smooth muscle α-actin (brown; D, G) and Caspase-3 (brown; E, H) stainings are shown. Note that the more complex construct in the upper row requires more time to fuse.

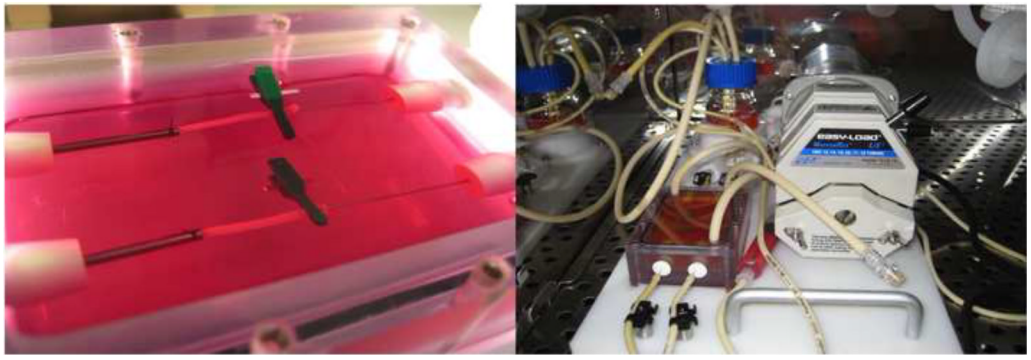

Fig. 7.
Maturation of bioprinted tubes composed of porcine aortic smooth muscle cells (left) in a perfusion bioreactor (right).

NIH-PA Author Manuscript
NIH-PA Author Manuscript
NIH-PA Author Manuscript